April 2008 Volume 4 Issue 3

Trade Science Inc.

Materials Science

An Indian Journal

Full Paper

MSAIJ, 4(3), 2008 [185-192]

Determination of the real global or local carbon contents in a high temperature alloy by using thermodynamic calculations

Patrice Berthod

Laboratoire de Chimie du Solide Mineral (UMR 7555), Faculte des Sciences et Techniques, UHP Nancy 1, Nancy-Universite BP 239, 54506 Vandoeuvre-les-Nancy, (FRANCE)

E-mail : Patrice.Berthod@lcsm.uhp-nancy.fr

Received: 11th February, 2008 ; Accepted: 16th February, 2008

ABSTRACT

Oxidation of the molten bath during oxidation, as well as oxidation in service at high temperature can lead to a global or a local impoverishment of the carbon contained in an alloy. The determination of the carbon content was achieved by using thermodynamic calculations first for a Co(bal.)-Cr-C-Ta alloy elaborated by foundry in a not totally inert atmosphere, and second after oxidation for 50 hours at 1,000°C, 1,100°C and 1,200°C. The association of metallographic quantifications, micro-analysis measurements and calculated results with iterations about the carbon content, allowed to assess the loss of all the elements during casting and to specify the new distribution of carbon in the sub-surface affected by oxidation.

KEYWORDS

High temperature;
Oxidation;
Thermodynamic calculations;
Carbon.

INTRODUCTION

Among the solutions of mechanical reinforcement for the cast alloys and superalloys employed at high temperature, there is the strengthening by carbides[1,2]. These ones can be primary carbides (appeared during solidification) and secondary carbides (obtained by applying a specific heat treatment to the alloy). These can be of different varieties (M_7C_3, $M_{23}C_6$ or MC for example), this depending on the chemical composition of the alloy, the contents' ratio of carbon and the carbide-forming metallic elements.

Achieving a strengthening by carbides supposes the introduction of carbon in the charge before or during the melting which can be achieved in an inert atmosphere or simply in air. In the second case, it is not always easy to obtain the targeted carbon content because this element tends to react with oxygen at high temperature and it disappears in gaseous species. In addition the same problem is generally encountered for the metallic carbide-forming elements, such as Ti or Ta for instance, with formation of solid oxides which segregate to the surface of the bath. Finally this can lead to real compositions of alloys that are not very close to the targeted ones, which can have significant consequences for the types and volume fractions of the obtained carbides and then for their strengthening effect.

Secondly, when they are used in oxidizing atmospheres, the alloys for high temperature applications undergo an oxidation of their surface which involves modifications of their chemical composition and their microstructure in a more or less deep zone from the external

surface. Generally carbides tend to disappear in the sub-surface while some new carbides sometimes precipitate between this appearing carbide-free zone and the bulk. These phenomena are related to the diffusion of the elements which initially belonged to the carbides, i.e. carbon and the carbide-forming elements.

Thus, because of the phenomenon of high temperature oxidation, undergone by the liquid alloy during its elaboration or by the solid alloy during its use, general or local changes of the chemical composition of the alloy can be induced. They can be evaluated by microanalysis measurements for the contents of the metallic elements, while it is often not possible, or at least more difficult, for carbon which is a too light element although it is of great importance for the mechanical properties. Fortunately, indications about the carbon real contents can be obtained by fitting a microstructure state obtained after a sufficiently long exposure at a constant high temperature by iterative thermodynamic calculations for varying contents of carbon. In this work two examples are treated with a same cobalt-base alloy. Firstly this alloy obviously lost a part of its carbon during its elaboration by casting because a not totally inert atmosphere above the bath, and it was attempted to better know the real carbon content which was finally obtained in the solidified alloy, by using thermodynamic calculations. Secondly, after several tens hours of exposure to high temperature in an oxidizing atmosphere, microstructure modifications occurred in the sub-surface of this alloy. They can be related to a local new distribution of carbon due to high temperature oxidation which can be also better known thanks to thermodynamic calculations.

EXPERIMENTAL

Choice and elaboration of the alloy of the study

The alloy which was considered here is a cobalt-base alloy, belonging to the same family as some cast industrial alloys for high temperature applications. But it has a more simple composition since it only contains cobalt (the base element, about 60 wt. % of the whole alloy), chromium (to resist hot corrosion but also which is a carbide-forming element, targeted content 30 wt.%), tantalum (which is also a carbide-forming element, but stronger than Cr, targeted content 6 wt.%), and carbon (targeted content 0.4 wt.%). The obtained chemical composition is given in TABLE 1. This alloy was synthesized from pure elements (99.9%, Alfa Aesar), using a high frequency induction furnace, in order to get an ingot of about 100g. It was melt under a partially inert atmosphere (mainly argon but with the possible presence of residual air), in order to limit a possible oxidation of the elements during heating and melting. Fusion and solidification were achieved in a copper crucible cooled by circulation of water. The obtained ingot was cut in order to get, firstly a small part to measure the temperature intervals of fusion and solidification, and secondly more important parts for the study of stable microstructures at high temperature.

TABLE 1: Chemical composition of the studied alloys measured in the obtained alloy by microanalysis (3 EDS measurements, average value ± standard deviation)

Elements	Contents (wt.%)
Co	bal.
Cr	29.31± 1.98
Ta	4.23± 0.39
C	unknown(but lower than 0.4)

Determination of the solidus and liquidus temperatures

The solidus and liquidus temperatures of the alloy was determined by performing Differential Thermal Analysis (DTA) experiments from a 2×2×7 mm^3 sample, using a Setaram TGA 92-16.18 apparatus. The thermal cycle was composed firstly by a heating rate of 20K min^{-1} up to 1,200°C then by a slower heating at 5K min^{-1} up to 1,500°C for a better accuracy for this level of temperature, and secondly by a cooling at 5K min^{-1} down to 1,200°C, then at 20K min^{-1} down to room temperature. Beginnings and ends of fusion and solidification were determined. The solidus temperatures (respectively liquidus temperatures) were supposed to be close to the average value of the temperatures of the beginning (respectively end) of fusion and of the end (resp. beginning) of solidification.

High temperature exposure and metallographic characterization

Three 10×10×3mm^3 samples were cut from the ingot, and polished with 1200-grit paper. The samples were exposed for 50 hours in a Setaram TGA 92

thermobalance at 1,000, 1,100 and 1,200°C under air at atmospheric pressure. The heating was done at 20K min^{-1} and, at the end of the 50 hours stage at high temperature, the cooling to room temperature was done at 10K min^{-1}. The microstructures were examined in embedded samples. These ones were prepared by cutting the samples with a Buehler Isomet 5000 precision saw, and by embedding them in a mold using a cold resin mixture (Escil CY230 + HY956). They were polished using SiC paper from 120 to 1,200 grit under water, and finally with a 1µm diamond paste.

The chemical composition of the alloy was measured by using the Energy Dispersion Spectrometry device of a Scanning Electron Microscope (SEM, type: XL30 Philips), only for Co, Cr and Ta, since carbon cannot be analyzed because of its too low atomic weight. Three measurements were done in three different places in the middle of the sample's bulk, i.e. far from the zone affected by oxidation. The three analyzed areas were about 0.5mm² (magnification×125), and the average weight content was calculated for each element.

Metallographic observations were done with the SEM in the Back Scattered Electrons mode with a 20kV acceleration voltage. The region of interest for the characterization of the stable microstructures at the three temperatures was also the middle of the sample's bulk. The chemical compositions of carbides were measured with a CAMECA SX100 microprobe (pinpoint microanalysis). The surface fractions of carbides were measured on three BSE micrographs taken on each sample with the SEM in BSE mode, in three different locations randomly chosen (magnification×1,000, areas of almost 0.005mm²). The BSE detector leads to different levels of gray, depending on the average atomic number of the considered phase. This allowed to separate the pixels of matrix (gray), of chromium carbides (darker than matrix), and of tantalum carbides (white). The carbides surface fractions were measured using the Photoshop CS software of Adobe. This was done on the three micrographs files of a same sample, and each final surface fraction, average of three measures, was supposed to be close to the volume fractions.

Thermodynamic calculations

The calculations of all the theoretic liquidus and solidus temperatures, natures and mass fractions of carbides, and chemical compositions of matrixes, were performed using the Thermo-Calc version N software[3] with the SSOL database[4] to which the descriptions of some missing systems were added: Ta-C[5], Co-Ta[6], Cr-Ta[7] and Co-Ta-C[8]. The calculated mass fractions of carbides were converted in volume fractions according to $f_v[\phi_j] = (f_w[\phi j]/\rho_{\phi j}) / \sum_i (f_w[\phi_i]/\rho_{\phi i})$, in which $f_v[\varphi_j]$, $f_w[\varphi_j]$ and $\rho\varphi_j$ are respectively the volume fraction, the mass fraction and the density of the phase φ_j. The values of the densities which were taken for these calculations were 7.95g cm^{-3} for matrix (obtained by direct measurement on a Co-30Cr sample), 6.941g cm^{-3} for Cr_7C_3, 6.953g cm^{-3} for $Cr_{23}C_6$ and 14.5g cm^{-3} for TaC[9].

RESULTS AND DISCUSSION

Determination of the carbon content of the alloy

The microstructures of Alloy 1 after 50 hours of exposure at the three high temperatures, illustrated in Figure 1 (magnification×1,000), are characterized by a dendritic austenitic matrix of Co-solid solution and carbides which are almost exclusively TaC carbides (clearly identified by microanalysis). Some of them are interdendritic primary carbides and they obviously form

After 50 hours at 1,000°C; After 50 hours at 1,100°C; After 50 hours at 1,200°C

Figure 1: Microstructures after 50 hours at 1,000, 1,100 or 1,200°C (SEM pictures in BSE mode)

a eutectic compound with matrix. These primary carbides seem to be less present and rounder for 1,200°C than for the two lowest temperatures. The other TaC carbides are intragranular secondary very fine carbides which obviously precipitated in the matrix during the stage at high temperature, essentially in the cases of the two lowest temperatures. Another type of carbide can also be seen in the samples, but their quantities are very lower than for TaC. They seem to be chromium carbides but their too small sizes did not allow their identification by microanalysis. Surface analysis were performed on three micrographs taken with the SEM in BSE mode at the magnification×1,000 and TABLE 2 presents the values obtained for the surface fractions of the two types of carbides. The TaC carbides (about 2 vol.%) are effectively the main carbide phase. Chromium carbides, which are already rare for 1,000°C, have almost disappeared for the two highest temperatures. The surface or volume fraction of the tantalum carbides slightly decreases when the stage temperature increases.

Global EDS microanalysis were performed of three 0.5mm² areas in each sample, and this led to similar chromium and tantalum contents, which are already displayed in TABLE 1 above. The obtained contents are, for chromium a little lower than expected (30wt.% Cr), and for tantalum significantly lower than targeted (6wt.% Ta). Oxidation during heating and melting obviously induced a partial lost of these two elements for the final alloy. Concerning carbon, which cannot be analyzed, it seems that its content is sensibly lower than the targeted one (0.4wt.%C) since the obtained carbides are essentially TaC although the tantalum content has fallen to near 4wt.% instead of 6 wt.%.

With the measured value of the weight content of tantalum (4.23wt.%), significantly decreased from the targeted value (6wt.%), one can think that chromium carbides ought to be present in the microstructure with higher volume fractions than really observed in the samples. This can be confirmed by Thermo-Calc calculations which may lead, for the Co-29.31Cr-4.23Ta-0.4C composition, to volume fractions (after conversion of the mass fractions given by Thermo-Calc) that are 2.60vol.% $M_{23}C_6$ and 2.22 vol.% TaC for 1,000°C, 2.15 vol.% $M_{23}C_6$ and 2.17 vol.% TaC for 1,100°C, and 1.32 vol.% $M_{23}C_6$ and 2.12 vol.% TaC for 1,200°C. Then, the carbon content was certainly also decreased because of oxidation during the elaboration of the alloy, and the obtained microstructures which were observed and characterized in terms of carbides fractions allow to deduce a probable value of carbon content, with the help of thermodynamic calculations. For that, calculations were performed for several compositions Co(bal.)-29.31Cr-4.23Ta-xC with x varying from 0.25wt.% to 0.40wt.%, for the three temperatures 1,000, 1,100 and 1,200°C. The calculated mass fractions of the two types of carbides, TaC and $Cr_{23}C_6$ were converted in volume fractions and plotted versus the theoretic carbon weight content in figure 2. Then, for each temperature and each type of carbide, it is possible to specify the carbon content leading to the measured value of volume fraction of this carbide, as

TABLE 2: Surface (or volume) fractions of the carbides in the bulk at the three temperatures, measured by surface analysis (average value ± standard deviation)

Carbides fractions(vol.%)	TaC	$M_{23}C_6$
1200°C	2.08 ± 0.17	0.01± 0.01
1100°C	2.11± 0.26	0.02± 0.01
1000°C	2.21± 0.05	0.16± 0.10

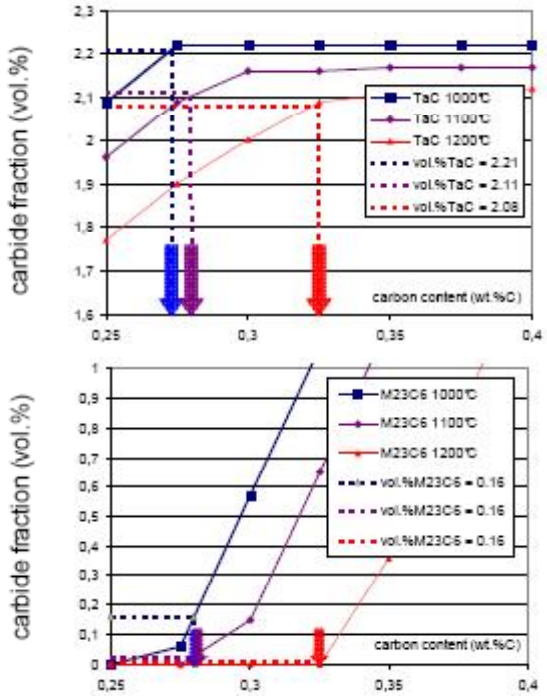

Figure 2: The TaC carbide fraction and the $M_{23}C_6$ carbide fraction plotted versus the carbon content for the three temperatures (Thermo-Calc calculations); determination of the real carbon content from the measured carbide fractions (broken lines and arrows)

illustrated by the broken lines in the two graphs of figure 2. It was much more easy to do and the result much more precise for the TaC phase than for the $M_{23}C_6$ phase, since the former was more present than the latter. This led to the carbon contents displayed in TABLE 3, which are close from one another, and the average value of which is 0.30 wt.% C. So, it seems that about 0.1 wt.% (i.e. a quarter of the carbon mass) of the carbon initially present as graphite parts in the charge to melt, was oxidized during the elaboration of the alloy and quitted the furnace as gas.

A DTA experiment was performed on the alloy to measure the temperatures of beginning and of end of fusion, in order to verify if there is a good correspondence of these temperatures and the solidus and liquidus temperatures that can be calculated from the supposed chemical composition Co(bal.)-29.31Cr-4.23Ta-0.30C. The DTA curve and the results are given in figure 3 and TABLE 4. With a difference of about 10°C between the experimental values and the calculated values, one can reasonably consider that there is a good agreement, even if it is not perfect. This confirms that the carbon content is really 0.30 wt.%C or at least very close to this value.

Assessment of the new carbon distribution in the sub-surface after oxidation

Figure 4 presents the microstructures of the sub-surfaces after exposure at the three temperatures. The oxidized samples all display an external chromia scale (average thicknesses equal to 8µm for 1,000°C, 10 µm for 1,100°C and 16µm for 1,200°C), sometimes mixed by tantalum and chromium oxides films. Internal

TABLE 3: Possible values for the carbon content, deduced from the carbides fractions

from the vol.% of TaC at 1,100°C	from the vol.% of $M_{23}C_6$ at 1,100°C	from the vol.% of TaC at 1,200°C	from the vol.% of $M_{23}C_6$ at 1,200°C
0.29	0.29	0.32	0.33
From the vol.% of TaC at 1,000°C	From the vol.% of $M_{23}C_6$ at 1,000°C	Average value:	0.30
0.27	0.28		

TABLE 4: Average temperatures of fusion's beginning and solidification's end, and of solidification beginning and fusion's end (DTA); comparison with the temperatures of solidus and of liquidus calculated by Thermo-Calc

Temperature of liquidus (°C)	
DTA (average heating + cooling)	Th.-Calc
1403	1392
Temperature of solidus (°C)	
DTA (average heating + cooling)	Th.-Calc
1302	1309

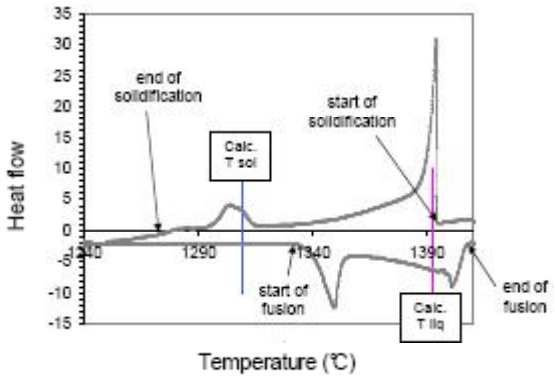

Figure 3: DTA curve with positions of the beginnings and ends of fusion and solidification; comparison with the temperatures of solidus and of liquidus calculated by Thermo-Calc (the two vertical lines)

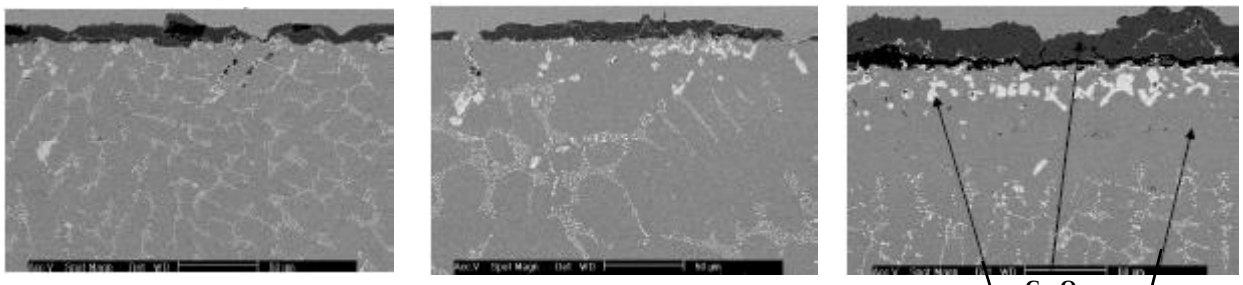

After 50 hours at 1,000 °C **After 50 hours at 1,100 °C** **After 50 hours at 1,200 °C**

Figure 4: Sub-surface states after 50 hours at 1,000, 1,100 and 1,200°C (SEM pictures in BSE mode)

Full Paper

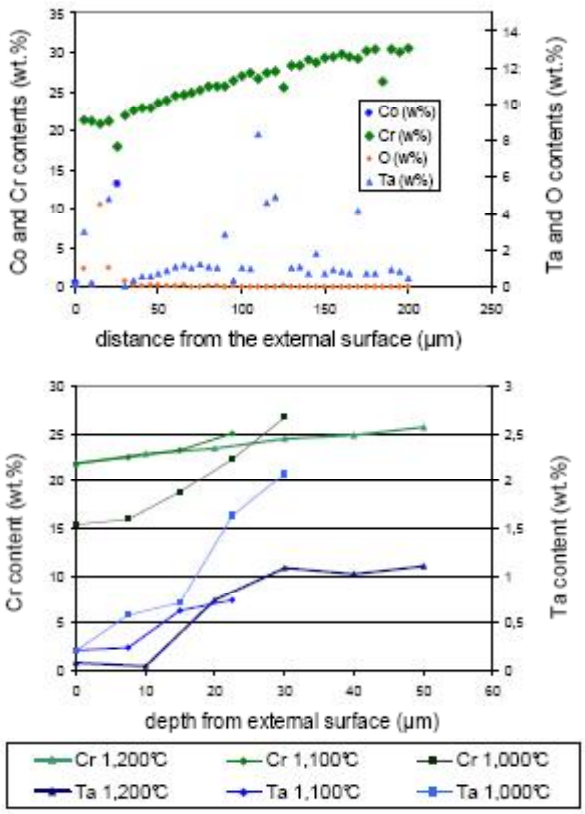

Figure 5: Top: example of WDS contents profiles (performed on the sample oxidized 50 hours at 1,200°C); bottom: depletions of the Cr and Ta contents in the carbide-free zones for all samples

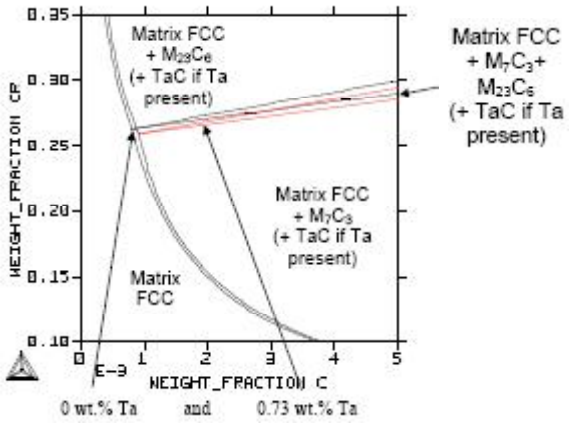

Figure 6: The two superposed isothermal sections (T = 1,100°C) corresponding to 0.73 and 0 wt.%Ta

oxidation can also be seen in the sub-surface (oxides of both Cr and Ta too) where one also sees a zone in which carbides disappeared and which is deeper when the temperature of exposure is higher (average depths equal to 11µm for 1,000°C, 29µm for 1,100°C and

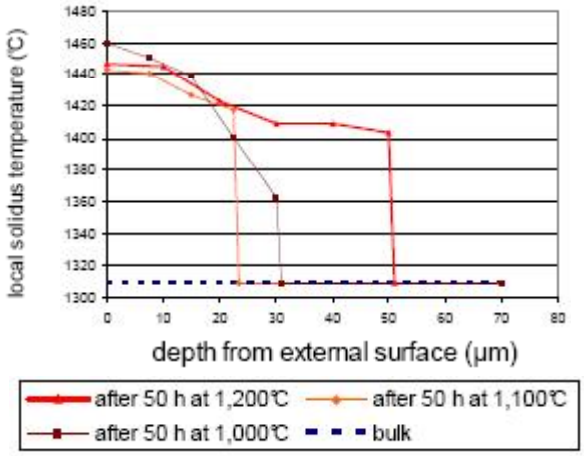

Figure 7: Plots of the solidus temperatures versus the depth across the carbide-free zones obtained after 50 hours at 1,000°C, 1,100°C and 1,200°C (results calculated from the Ta and Cr contents at each depth according to the WDS profiles)

67µm for 1,200°C). WDS profiles performed across the sub-surface zone affected by oxidation show an impoverishment in both chromium and tantalum from the bulk to the external surface, as illustrated by figure 5 with real WDS profiles for the sample oxidized at 1,200°C, and for Cr and Ta only across the carbide-free zones for the three temperatures together.

The presence of carbon in an alloy containing chromium with or without tantalum easily leads to the existence of carbides at the equilibrium for temperatures comprised between 1,000 and 1,200°C, even if the C content is not high. However it is true that very small quantities of carbon are compatible with a FCC-matrix monophased state, as demonstrated for 1,100°C (i.e. the intermediate temperature) by figure 6 for the two extreme values of the Ta content in the WDS profiles performed across the carbide-free zone obtained in the alloy for this temperature, i.e. 0 at the extreme surface and 0.73wt.% Ta at the frontier separating the carbide-free zone and the area where carbides still exist. More precisely, for 1,100°C the carbon content is necessarily decreased to at least 0.1wt.%C in the carbide-free zone (a content limit which is few dependent on the real Ta content between 0 and 0.73 wt.%), and probably to 0 wt.% since the very little carbon atoms have certainly diffused quicker than Ta and even Cr towards the oxidation front.

The development of a carbide-free zone, in which

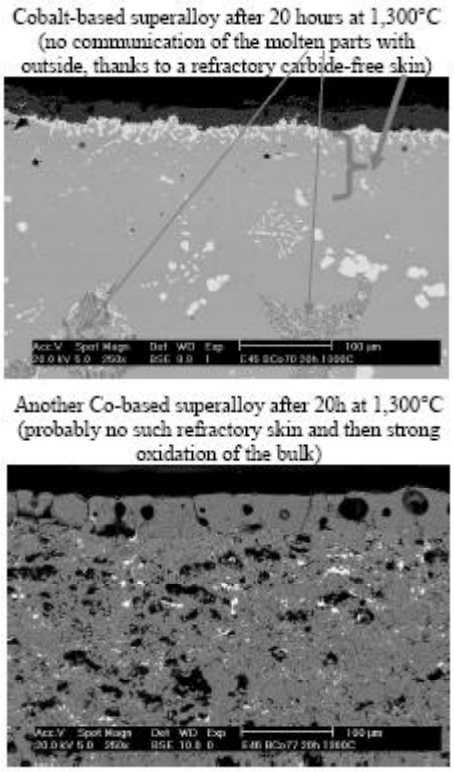

Figure 8: Oxidation in air at 1,300°C of two Co-based superalloys having solidus temperatures lower than 1,300°C; the first one (left hand) was protected from the oxidizing atmosphere by the still solid carbide-free zone, while the bulk of the second one (right hand) was catastrophically oxidized because of the absence of such refractory barrier

no carbides - then no eutectic carbides - are still present and which is impoverished in alloying elements (Ta and Cr), can be considered as being a metallic outer part of the alloy, which is especially refractory. Indeed, if the carbon content can be supposed to be almost zero, the knowledge of the Cr and Ta contents measured by microanalysis (WDS profiles) allows determining a local solidus temperature by using thermodynamic calculations. This was done here from the simplified Ta and Cr profiles (limited to the carbide-free zone area) presented together in the second graph of figure 5 (for the three temperatures of exposure). The graph given in figure 7, (corresponding to the hypothesis of a carbon content equal to zero everywhere in the carbide-free zone), which contains the three curves which represent the evolution of the local solidus temperature versus the depth from the external surface, effectively shows that the local solidus temperature is near one hundred higher than the bulk's one.

General commentaries

The atmosphere not perfectly inert in which the elaboration of the alloy was achieved effectively caused a loss of the more oxidable elements belonging to the chemical composition of the alloy. The chromium content was slightly decreased (loss of almost 1 wt.%Cr), but the loss especially concerns tantalum (loss of almost 2 wt.%) and also carbon since the metallographic characterization coupled with thermodynamic calculations showed that about 0.1 wt.%C, as is to say 25% of the initial carbon mass in the charge, has gone away into gaseous species. Despite of the decrease in tantalum, the carbides present in the microstructure were essentially TaC carbides, as initially expected with the choice of both 6 wt.% Ta and 0.4 wt.%C, since the appearance of less refractory other carbides, i.e. chromium carbides, was avoided by the decrease of carbon. Nevertheless, the TaC volume fraction is decreased, this inducing consequently a probable weakness of the mechanical strength at high temperature[10]. In addition some rare chromium carbides, supposed being $M_{23}C_6$ as shown by calculations (these carbides are too small to be analyzed by microprobe), are also present.

The graphs of variation of the carbide fraction versus the carbon content (Figure 2), initially plotted in order to specify the real carbon content in the alloy, are also interesting for other considerations. Firstly they showed that the fractions of the two types of carbides increase with the carbon content and decrease when the temperature increases, as experimentally observed with image analysis. Secondly, the carbide-forming power of tantalum which is stronger than the chromium's one is revealed by the priority of TaC formation when the carbon content increases. From the lowest carbon contents, each increase in C content is profitable to the TaC formation, until the Ta content in matrix has sufficiently decreased. Thereafter, each new increase in C content promotes an increase in $Cr_{23}C_6$ carbides. The carbon content of transition from the increase in TaC to the increase in $Cr_{23}C_6$ is all the more high since the temperature is high. Depending on the level of the carbon content, either the tantalum carbide fraction or the chromium carbide fraction leads to the carbon content in the alloy.

Full Paper

Concerning the effect of the high temperature oxidation, the development of a carbide-free zone due to the diffusion, towards the external surface, of the carbide-former elements which are also the most oxidable elements of the chemical composition of the alloy, implies that carbon is also lost in this part of the alloy. Obviously it quitted the alloy, oxidized into gaseous species, since no coarsening or precipitation of new carbides obviously occurred along the frontier between the carbide-free zone and the bulk, as sometimes observed in other carbides-strengthened alloys or superalloys oxidized at such temperatures[11,12]. The disappearance of carbon from this carbide-free zone can have important consequences. A first one is the presence of an alloy's external part which has an average solidus temperature which is significantly increased, more precisely about one hundred degrees higher than the bulk's one. This means that a sudden increase in temperature can accidentally occur without partial melting of this external part. Then, in such a situation, if the bulk begins to melt, the molten areas all remains internal. A second one is a best separation of the oxidizing atmosphere and the most oxidable phases present in the alloy, i.e. chromium carbides and tantalum carbides. After several tens hours at moderate temperatures (e.g. 1,000 or 1,100°C), the obtained carbide-free zone can act as a temporary barrier which is able to protect, from oxidation at higher temperatures, either the interdendritic carbides or the molten Cr and Ta-rich interdendritic areas (depending on the value reached by the temperature), in case of sudden increase of temperature (example in figure 8). Of course, this barrier can be rapidly lost because of its enhanced oxidation on its external side, and diffusion of elements from the bulk solid or partially molten, on its internal side.

CONCLUSIONS

Casting in not totally inert atmospheres can lead to the impoverishment in the most oxidable elements. This lost can be known for all elements by spark spectrometry for example, or using micro-analysis measurements for the elements that are not too light or too rare in the alloy. Thermodynamic calculations can also be considered as an indirect mean for determining the content of the lightest elements, such carbon, when other apparatus allowing their measurement is not available. However, for that, performing sufficiently long exposures at high temperature to be sure that the thermodynamic equilibrium is effectively reached, is necessary and unfortunately time-consuming. Thermodynamic calculations are also very useful to assess carbon contents where local microstructure modifications possibly involving changes of carbon contents can be noticed. It is the case of phenomena induced by oxidation at high temperature which can modify the properties of the outer part of the alloy.

REFERENCES

[1] E.F.Bradley; 'Superalloys: A Technical Guide', ASM International; Metals Park, **(1988)**.

[2] C.T.Sims, W.C.Hagel; 'The Superalloys', John Wiley & Sons, New-York, **(1972)**.

[3] Thermo-Calc version N: 'Foundation for Computational Thermodynamics', Stockholm, Sweden, Copyright, www.thermocalc.com, **(1993, 2000)**.

[4] SGTE: Scientific Group Thermodata Europe database, update, **(1992)**.

[5] K.Frisk, A.Fernandez Guillermet; J.All.Compds, **238**, 167 **(1996)**.

[6] Z.-K.Liu, Y.A.Chang; Calphad, **23**, 339 **(1999)**.

[7] N.Dupin, I.Ansara, J.Phase Equilibria; **14**, 541 **(1993)**.

[8] L.Dumitrescu, M.Ekroth, B.Jansson; Metall.Mater. Trans.A, **32A**, 2167 **(2001)**.

[9] 'Handbook of Chemistry and Physics', 57th edition **(1976-1977)**.

[10] P.Berthod, J.L.Bernard, C.Liebaut ; Patent WO2001090429.

[11] P.Berthod S.Michon, S.Mathieu, R.Podor, P. Steinmetz; Mater.Sci.Forum, **461-464**, 1117 **(2004)**.

[12] P.Berthod, C.Vebert, L.Aranda, R.Podor, C.Rapin; Oxid.Met., **63(1/2)**, 57 **(2005)**.